R. & M. No. 1913
(7153 & 7365)
A.R.C. Technical Report

MINISTRY OF SUPPLY

AERONAUTICAL RESEARCH COUNCIL
REPORTS AND MEMORANDA

Effect on Aerofoil Drag of Boundary-Layer Suction Behind a Shock Wave

By

A. FAGE, F.R.S., and R. F. SARGENT
of the Aerodynamics Division, N.P.L.

LONDON: HIS MAJESTY'S STATIONERY OFFICE
1949
Price 4s. 0d. net

Effect on Aerofoil Drag of Boundary-Layer Suction Behind a Shock Wave

By

A. FAGE, F.R.S., and R. F. SARGENT
of the Aerodynamics Division, N.P.L.

Reports and Memoranda, No. 1913
26th October, 1943

Summary.—(*a*) *Reasons for Enquiry.*—To measure, at Mach numbers near the critical value, the reduction in drag due to boundary-layer suction on the upper surface of an aerofoil. To determine whether this reduction can be obtained with an economic use of power.

(*b*) *Scope of Investigation.*—The experiments were made on 2 in. chord aerofoils, NACA 0020 section, at 0 deg. and 4 deg. Drag was determined from pitot tube traverses at one chord behind the trailing edge of the model. Information on the flow over the upper surface was obtained from pitot tube traverses at 0·02 chord behind the trailing edge, from visual observation of shock waves, from surface tube observations just forward of the slot, and from normal pressure measurements. The cases considered are those for which shock waves cause boundary-layer separation and those for which shock waves are not present or are too weak to cause separation. Estimates of the power absorbed by the compressor, ignoring duct losses, are obtained from (i) measurements of the mass of air sucked and the maximum stagnation pressure of the air issuing from the slot, and (ii) a boundary-layer relation which includes entry shock losses but not the losses in the slot.

(*c*) *Results.*—Suction has little effect on the critical Mach numbers, $M_c = 0{\cdot}65$ for $\alpha = 0$ deg. and $0{\cdot}57$ for $\alpha = 4$ deg., but the minimum drags with suction on the upper surface are 40 per cent., $\alpha = 0$ deg., and 50 per cent., $\alpha = 4$ deg., lower than the aerofoil drags without suction, $0{\cdot}45 < M < 0{\cdot}735$. The drag coefficients measured at the critical Mach numbers without suction are obtained with suction at Mach numbers which are $0{\cdot}08$, $\alpha = 0$ deg., and $0{\cdot}105$, $\alpha = 4$ deg., higher. The drag falls to its minimum value when about 0·6 of the mass of air in the boundary layer is sucked. In the present experiments, the power saved by the reduction in drag due to suction is about the same as the estimated power absorbed by the compressor.

(*d*) *Conclusion.*—The experiments give promise that, at the Reynolds numbers of flight and for an efficient slot and suction system, the drag coefficient of a wing at the critical Mach number without suction can be maintained at the same value and with an economic use of power to a higher Mach number, say $0{\cdot}1$ higher, by boundary-layer suction.

1. *Introduction.*—The rapid rise in the drag coefficient of an aerofoil which occurs with an increase in speed beyond that at which shock waves are formed is associated with losses of mechanical energy across the shock waves and with the effect of the shock waves on the boundary layer. If the pressure gradients across the shock waves are sufficiently large the boundary layer separates from the surface, and complete separation downstream of the shock waves may occur. The inevitable drag increase due to losses of mechanical energy across the shock waves can therefore be augmented by losses due to boundary-layer separation.

Theoretical considerations lead to the conclusion that, with an increase in Mach number above the critical value, the drag due to energy losses across a shock wave is at first small, and that this drag increases at a smaller rate than the measured total drag[1, 2]. It appears, therefore, that economic flight of an aeroplane beyond the critical Mach number of its wings might be possible if boundary-layer separation were prevented.

Boundary-layer separation due to a shock wave can be prevented by removal of the inner part of the layer by suction behind the wave. The experiments now to be described have been made to obtain a measure of the reduction in drag to be expected from this method of preventing separation, and to find out whether the reduction can be obtained with an economic use of power. The effects of boundary-layer suction at Mach numbers near the critical value for which shock waves are not formed, or, if formed, are too weak to cause boundary-layer separation are also considered.

2. *Notation.*

α	aerofoil incidence,
c	aerofoil chord,
x	distance along the chord from the leading edge,
y	distance normal to the aerofoil surface, or the lateral distance across wake, or the distance normal to axis of the slot, or the distance normal to the axis of the discharged jet,
s	distance along the aerofoil surface from the stagnation point,
t	width of slot,
U_0	velocity of the undisturbed stream,
a_0	velocity of sound in the undisturbed stream,
M	Mach number $\frac{U_0}{a_0}$,
M_c	critical Mach number at which the drag coefficient begins to rise,
p_0	pressure of the undisturbed stream,
ρ_0	density of the undisturbed stream,
ν_0, μ_0, E_0, T_0	kinematic viscosity, viscosity, total energy per unit mass and temperature in the undisturbed stream,
μ_W	viscosity at the surface,
p_A, ρ_A, T_A	atmospheric pressure, density and temperature,
u, p, ρ	velocity, static pressure and density inside the boundary layer, or at any point in the field of flow, p is also the surface pressure,
$u_1, p_1, \mathscr{R}$	velocity, pressure and density just outside the boundary layer,
u_2, p_2, ρ_2	velocity, static pressure and density behind the shock wave at the entry to the slot,
u_3, p_3, ρ_3	velocity, static pressure and density in the slot,
u_4, p_4, ρ_4, T_4	velocity, static pressure, density and temperature in the discharged jet,
u_s	surface tube velocity,
H	stagnation pressure in the wake,
H_3	stagnation pressure of the air in the slot,
H_c	peak stagnation pressure of the air in the slot,
T_j	thrust due to the jet reaction per unit span,
γ	ration of the specific heat of air at constant pressure to the specific heat at constant volume,
δ	boundary-layer thickness,
δ^*	displacement thickness of the boundary layer $\int_0^\delta \left(1 - \frac{\rho}{\mathscr{R}} \frac{u}{u_1}\right) dy$,
θ	momentum thickness of the boundary layer, $\int_0^\delta \frac{\rho u}{\mathscr{R} u_1}\left(1 - \frac{u}{u_1}\right) dy$,
Y	width of the boundary layer sucked into the slot,
Λ	$= \frac{\delta^2 \mathscr{R} u_1'}{u_W}$,
D	profile drag per unit span measured by the pitot-traverse method, without boundary-layer suction,
D_s	profile drag per unit span, with boundary-layer suction,
D_1	effective drag per unit span,

m_b	mass flow in the boundary layer per unit span per sec. at the slot position,
m_s	mass of air sucked per unit span of the slot per sec.,
ε	work done per second on the air flowing through unit span of the slot to raise the pressure to p_0 and the velocity to U_0,
P	power absorbed by the compressor,
ε_f	work done per sec. per unit span of the slot against the friction in the duct system (excluding compressor),
η	efficiency of the main propulsive system,
η_1	compressor efficiency,
τ	intensity of the surface friction,
ζ	$(\mathscr{R}u_1^2/\tau)^{\frac{1}{2}}$,
$F(\zeta)$	$10{\cdot}411\zeta^{-2}\, e^{-0{\cdot}3914\zeta}$,
C_p, C_D, C_{Ds}, C_{D1}, C_ε, $C_{\varepsilon f}$	absolute coefficients.

3. *Experiments.*—The experiments were made on two models, 2 in. chord and 2 in. span. The 20 per cent. thick symmetrical section NACA 0020, was chosen to obtain shock waves at low incidences, 0 deg. and 4 deg., at speeds well below the highest speed of the tunnel. A forward-facing suction slot with faired lips was cut in one surface, the upper surface for $\alpha = 4$ deg., of each model, *see* Fig. 1b. The entry to the slot was at $x = 0{\cdot}5c$. The slot was $0{\cdot}035$ in. wide and its axis was inclined at 45 deg. to the chord. Each model was mounted between the 5 in. walls of the 5 in. $\times$ 2 in. high-speed tunnel described in Ref. 3. The tunnel had flexible walls, suitably shaped to minimise wall interference. Shape ordinates of the upper surface of each model, designated I and II, are given in Fig. 1. Model I closely resembles the NACA 0020 shape. Model II is not so good as Model I : the maximum ordinate of the upper surface is 5 per cent. greater than that of NACA 0020 and is at $0{\cdot}35c$.

The datum velocity of the tunnel was determined from the static pressure measured at a hole in the side of the tunnel. This hole was two chords forward of the leading edge of the model. Aerofoil drag for the median section of Model I was determined by the standard National Physical Laboratory method,[4, 5] from total head and static pressure traverses at one chord behind the trailing edge. The drags obtained from traverses $\pm 0{\cdot}5$ chord from the median plane were sensibly the same as that for the median plane, so that the flow was two-dimensional. Pitot traverses were made at $0{\cdot}02$ chord behind the trailing edge of Model I to obtain information on the flow over the upper surface and on changes of flow due to suction. Details of the suction system are given in Appendix I and in Fig. 2.

Model II was used to obtain measurements of the normal pressure on the upper surface, with and without suction, and of the peak stagnation pressure, H_c, in the jet of air sucked into the aerofoil. The velocity, u_1, just outside the boundary layer was determined from the normal pressure by the standard relation for compressible flow, on the assumption that the pressure across the layer is constant and equal to the surface pressure. The peak stagnation pressure was measured by a small exploring pitot tube within the model, Fig. 1b. These experiments, and the method of estimating compressor power from H_c and the mass of air sucked, are described in Appendix IV. Velocity measurements very near the surface and just forward of the slot were also taken on Model II with a small surface tube of the Stanton type.

The pressure distributions measured on Model II without suction differ from the theoretical distribution for NACA 0020, because of the difference in sectional shape, but they suffice to show the effect of suction on the pressure distribution near the slot, and to allow an estimate of the rate of flow in the boundary layer. The difference in the theoretical and measured distributions of u_1/U_0, for $\alpha = 0$ deg. and $M = 0{\cdot}630$, is shown in Fig. 3a. The theoretical distribution for NACA 0020 was determined for the compressible flow pressure distribution, obtained from the incompressible flow pressure distribution[6] by the Temple-Yarwood relations given in Ref. 7.

4. *Drag Results.*—Figs. 3(b)–6(b) give measured curves of C_{Ds} against $m_s/\rho_0 U_0 c$ where C_{Ds} is the profile drag coefficient per unit span of the aerofoil with suction, m_s is the mass of air sucked into the slot per unit span per sec., ρ_0 and U_0 are the density and velocity of the undisturbed stream and c is the aerofoil chord. At first, C_{Ds} falls linearly with $m_s/\rho_0 U_0 c$, and then at a progressively slower rate until the minimum value is reached. The value of $m_s/\rho_0 U_0 c$ for $(C_{Ds})_{\min.}$ is somewhat indefinite. For the present analysis the value taken will be that obtained by producing the curve of linear fall of (C_{Ds}) to the measured value of $(C_{Ds})_{\min.}$, see dotted lines Figs. 3(b)–6(b).

Figs. 9 and 10 give curves of C_D and of $(C_{Ds})_{\min.}$ plotted against the stream Mach number M. The critical Mach numbers, M_c, for which the drag coefficient without suction begins to rise are taken to be $0{\cdot}65$, $\alpha = 0$ deg., and $0{\cdot}57$, $\alpha = 4$ deg.

These critical numbers are not sensibly affected by suction. For $\alpha = 0$ deg., $(C_{Ds})_{\min.}$ rises with increase in M above the critical value at about the same rate as C_D: for $\alpha = 4$ deg., the initial rate of rise in $(C_{Ds})_{\min.}$ is slower. For $\alpha = 0$ deg., $(C_{Ds})_{\min.}$ is about 40 per cent. lower than C_D, and for $\alpha = 4$ deg. about 50 per cent. lower, $0{\cdot}45 < M < 0{\cdot}735$. Consequently, for $\alpha = 0$ deg. the value of $(C_{Ds})_{\min.}$ for $M = 0{\cdot}73$ is the same as the value of C_D for $M_c = 0{\cdot}65$: for $\alpha = 4$ deg. the value of $(C_{Ds})_{\min.}$ for $M = 0{\cdot}675$ is the same as the value of C_D for $M_c = 0{\cdot}570$. In other words, the drag coefficients measured without suction at the critical Mach numbers are obtained with suction at Mach numbers which are about $0{\cdot}08$, $\alpha = 0$ deg., and $0{\cdot}105$, $\alpha = 4$ deg. higher. Further analysis of the drag results is given in § 8.

5. *Flow Pattern.*—The flows for which detailed analyses will be made are those for $\alpha = 0$, $M = 0{\cdot}630$ and $0{\cdot}735$, and $\alpha = 4$ deg., $M = 0{\cdot}681$ and $0{\cdot}730$. These cases are called I, II, III and IV respectively.

Information on the flows, with and without suction, for these cases was obtained from visual observation of shock wave position, from observations of surface pressure and from measurements of total head just behind the trailing edge. In addition, surface tube observations just forward of the slot were made without suction. For Case I, there are no shock waves, Fig. 3 (a). For Case II, there are shock waves on both surfaces, Fig. 4 (a). For cases III and IV, there are shock waves on the upper surface at about $0{\cdot}3c$ from the leading edge, Figs. 5 (a) and 6 (a). The position of the shock waves was not much affected by suction.

6. For Cases I–III, the regions over which the velocity u_1 is affected by suction extend from about $0{\cdot}2c$ to $0{\cdot}3c$ in front of the slot, to about $0{\cdot}15c$ behind, Figs. 3 (a)–5 (a). For Case IV, the region extends from about $0{\cdot}2c$ in front of the slot to the trailing edge of the model, Fig. 6 (a). Fig. 8 shows that the entire region beyond about $0{\cdot}2c$ forward of the slot is also affected by suction at the Mach number $0{\cdot}749$, $\alpha = 4$ deg., the change in u_1 due to suction being greater than that for $M = 0{\cdot}730$, Case IV, cf. Figs. 6 (a) and 8. It would appear therefore that for Case IV the boundary layer, without suction, beyond the shock wave position is separated from the surface. It is of interest to notice in Fig. 6 (a) that a marked change in the distribution of u_1/U_0 behind the shock wave occurs with a small increase in $m_s/\rho_0 U_0 c$ from $1{\cdot}1$ to $1{\cdot}45$: for intermediate values of $m_s/\rho_0 U_0 c$ the distribution was either that labelled $1{\cdot}1$ or that labelled $1{\cdot}45$; the former being obtained with an increase in suction and the latter with a decrease.

Figs. 3 (c)–6 (c) give distributions of $(p_A - H)/(p_A - p_0)$, where p_A is the atmospheric pressure, p_0 is the pressure in the undisturbed stream, and H is the total head measured at $0{\cdot}02c$ behind the trailing edge of Model I for $m_s = 0$ and for values of $m_s/\rho_0 U_0 c$ about the same as those for which C_{Ds} is a minimum. The curves for Case I confirm the visual observation that no shock waves are present. The curves for Case II clearly indicate the effect of shock waves on both surfaces, and those for Cases III and IV the effect of shock waves on the upper surface. Further, the peaks of the curves for Cases I and II, $m_s = 0$, are sharp and of the kind associated with boundary-layer flow which has not separated from the surface. For Case IV, $m_s = 0$, the peak of the curve associated with the flow over the upper surface is flat, an indication that the flow is separated from this surface. The curves for Cases II–IV show that the lateral extent of the shock waves has not been affected by suction.

7. The conclusions drawn from § 6 are that the boundary layers on the upper surface for Cases I and II, no suction, are not separated from the surface, and that the boundary layer for Case IV is separated from the surface behind the shock wave. More information on this matter was obtained from velocity measurements taken with a small surface tube of the Stanton type. The pitot tube was formed on the end of a 0·08 in. rod, Fig. 13, mounted on model II with the tube mouth at 0·433c behind the leading edge of the model. The external width of the tube mouth, *i.e.* the distance above the surface, was about 0·0035 in. Readings of $(p_s - p)$ and of $(p - p_0)$, where p_s is the stagnation pressure at the mouth of the surface tube, p is the static pressure taken at a hole in the surface of the model at a distance 0·433c from the leading edge, were taken at the two incidences, $\alpha = 0$ deg. and 4 deg. over a range of M from 0·62 to 0·74. Values of u_s/U_0 and of u_1/U_0, where u_s is the tube velocity, calculated from these pressure readings, are plotted against M in Fig. 13.

The values of u_s/u_1 for Cases I and II, Fig. 13a, are large and positive: there is, therefore, no boundary-layer separation at the tube position, *i.e.* 0·067c forward of the slot. The abrupt rise in the u_1/U_0 curve at $M = 0{\cdot}685$, for which u_1 is equal to the local velocity of sound, may be due to an interference effect of the static pressure tube on the reading of the static pressure hole. For Case II, $M = 0{\cdot}735$, there is a shock wave beyond the tube position and probably close to the slot.

Associated with the steep rise in u_1/U_0 at $M = 0{\cdot}685$ is an abrupt fall in u_s/u_1. The value of u_s/u_1 for Case II is about one-half of that for Case I. This lower value may be associated with a local thickening of the boundary layer.

The value of u_s/u_1 for Case I is 0·55. For a Blasius laminar boundary layer ($\Lambda = 0$) $u/u_1 = 0{\cdot}55$ when $y/\delta = 0{\cdot}25$, where u is the velocity at a distance y from the surface and δ is the boundary layer thickness. The value of δ at the tube position, if the boundary layer is laminar, is about 0·01 in. so that the effective distance, h_e, from the surface for which the velocity is equal to that calculated from the tube pressure is 0·0025 in. The value of h_e/h, where h is the width of the mouth, is 0·71.

For turbulent flow in the boundary layer, the value of h_e/h, estimated on the assumption that the velocity profile has the form $u/u_1 = (y/\delta)^{1/7}$, is 0·11. The value of the tube Reynolds number, $u_s h/\nu$, is about 560. Calibrations of small surface tubes, $h = 0{\cdot}0020$ in. and 0·0032 in. made for a range of low values of $u_s h/\nu$, 8 to 21 and 13 to 34 respectively, are given in Ref. 11. The values of h_e/h for $u_s h/\nu = 560$ obtained by extrapolation of these calibration curves, plotted on a logarithmic basis, are 0·65 and 0·55 respectively. The value of h_e/h obtained on the assumption of a laminar boundary layer has therefore the same order of magnitude as that to be expected from a direct calibration, whereas an improbably low value is obtained on the assumption that the flow is turbulent. It is to be inferred, therefore, that for Case I the flow in the boundary layer at the tube position tends to be of the laminar type.

The value of u_s/u_1 for Case III, $M = 0{\cdot}681$, is large and positive, Fig. 13b. The boundary layer is not separated, therefore, at the tube position, but the rapid fall of u_s/u_1 immediately beyond $M = 0{\cdot}681$ to a zero value at $M = 0{\cdot}705$ indicates that separation is imminent.

The surface tube reading for Case IV, $M = 0{\cdot}730$, is smaller than the static pressure on the surface, so that the boundary layer is completely separated from the surface at the tube position.

8. The drag of the rear half of the upper surface with suction, calculated for the measured distributions of u_1/U_0 for Cases I–IV on the assumption that there is no boundary-layer separation beyond the stagnation point on the rear lip of the slot, is 0·00065 $\rho_0 c U_0^2$, if the boundary layer is laminar, and 0·0015 $\rho_0 c U_0^2$, if it is turbulent. For Case I, the pitot-traverse drag of the upper surface for the condition C_{Ds} of the aerofoil a minimum, is 0·00058 $\rho_0 c U_0^2$, if the suction on the upper surface does not affect the drag of the under surface: for Case II, the pitot-traverse drag of the upper surface is 0·00155 $\rho_0 c U_0^2$. The pitot-traverse drag of the upper surface for Case I is therefore about the same as that calculated for laminar boundary-layer flow beyond the slot. For Case II, the pitot-traverse drag is about the same as the drag calculated for turbulent boundary-layer flow beyond the slot: but it cannot be inferred that the flow is turbulent,

because the pitot-traverse drag includes the mechanical losses due to the shock wave on the front half of the aerofoil. For Cases III and IV the pitot-traverse drags of the upper surface, for the condition C_{D_s} a minimum, are $0{\cdot}0026\ \rho_0 c U_0^2$ and $0{\cdot}0041\ \rho_0 c U_0^2$ respectively, if the pitot-traverse drag of the under surface, on which there are no shock waves, is taken to be the same as that for Case I (no shock wave). These estimates include the shock wave losses forward of the slot, so that if the flow in the boundary layer beyond the slot is laminar and if it has not separated from the surface the increments in drag due to these losses are about $0{\cdot}00195\ \rho_0 c U_0^2$ and $0{\cdot}00345\ \rho_0 c U_0^2$ respectively, that is, 21 per cent. and 20 per cent. of the aerofoil drag without suction.

9. *Values of δ and m_b.*—Detailed observation of boundary-layer flow could not be made because of the small size of the model, so that it was not possible to measure δ and m_b at the slot position, where m_b is the mass flow in the layer per second per unit span.

Rough estimates of these quantities have, however, been calculated for the measured distributions of u_1/U_0, for both laminar and turbulent flows at the slot position, on the assumption that the layer is not separated from the surface. For the turbulent flow at the slot it was assumed that transition occurs at $x = 0{\cdot}18c$ and that the velocity profile at the slot is given by $u/u_1 = (y/\delta)^{1/7}$. The results obtained are given in Table 2 (ii), Appendix II. The values of δ/c and $m_b/\rho_0 U_0 c$ for the laminar velocity profile are about one-half of those for the turbulent velocity profile. For Case I the flow at the slot is likely to be laminar and the value of m_s/m_b for the condition C_{D_s} a minimum is $1{\cdot}4$. For Cases III and IV the flow is turbulent and the value of m_s/m_b is about $0{\cdot}6$, on the assumption that the velocity profile is given by $u/u_1 = (y/\delta)^{1/7}$. These estimates do not, of course, take into account any effect due to boundary-layer separation upstream of the slot. For Case II, there is a thickening of the boundary layer at the slot due to the local shock wave. The value of m_s/m_b for C_{D_s} a minimum is difficult to estimate, because the state of the boundary layer at the slot is not known, but it may be about $0{\cdot}5$.

10. *Economy of Boundary-Layer Suction.*—The question now arises whether the reduction of drag by boundary-layer suction is obtained with an economic use of power. For two-dimensional subsonic flow past an aerofoil, with limited shock waves, the total drag when the air sucked into the aerofoil is discharged in the direction of its span is $D_s + m_s U_0$, where D_s is the profile drag per unit span measured by the pitot-traverse method and $m_s U_0$ is the sink drag per unit span, *see* Appendix III. Further, it is shown in Appendix III that, when the air is discharged backwards, the total power, *i.e.* the sum of the main propulsive power and the compressor power, needed to drive the aerofoil through the air with a velocity U_0 is

$$\frac{U_0}{\eta}[D_s + m_s U_0 - T_j] + \frac{1}{\eta_1}[\varepsilon + \varepsilon_f], \text{ where}$$

η is the efficiency of the main propulsive system,

η_1 is the compressor deficiency,

T_j is the thrust for unit span due to jet reaction,

ε is the work per second per unit span to raise the velocity and pressure of the air entering the slot to those in the jet exit, and

ε_f is the work done per second per unit span against the frictional resistance of the duct system, excluding that in the compressor.

For the present experiments a representative value of $m_s U_0$ for the condition D_s a minimum is $0{\cdot}0055\ \rho_0 U_0^2 c$. The sink drag is therefore large compared with the reduction in drag due to suction, but this sink drag can be neutralised by the thrust due to jet reaction, if the air sucked into the aerofoil is compressed adiabatically and discharged backwards with the velocity U_0 and the pressure p_0 of the undisturbed stream. We can therefore write $T_j = m_s U_0$. Further, on the assumption $\eta_1 = \eta$, the total power is $\frac{1}{\eta}[U_0 D_s + \varepsilon + \varepsilon_f]$.

The effective drag, D_1, of the entire system is then $D_s + \frac{1}{U_0}[\varepsilon + \varepsilon_j]$. Suction is beneficial if $D_1 < D$, that is, if $D_s + \frac{\varepsilon}{U_0} + \frac{\varepsilon_f}{U_0} < D$, that is, if $D - D_s - \frac{\varepsilon}{U_0} > \frac{\varepsilon_f}{U_0}$, where D is the drag per unit span without suction. Writing

$$C_D = \frac{2D}{\rho_0 c U_0^2}, \quad C_{D_s} = \frac{2D_s}{\rho_0 c U_0^2}, \quad C_\varepsilon = \frac{2\varepsilon}{\rho_0 c U_0^3} \text{ and } C_{\varepsilon f} = \frac{2\varepsilon_f}{\rho_0 c U_0^3},$$

this relation becomes $C_D - C_{Ds} - C_\varepsilon > C_{\varepsilon f}$. An estimate of the value of $C_{\varepsilon f}$ for the present duct system has not been obtained, because it is not one suitable for use in flight : but the value of $(C_D - C_{Ds} - C_\varepsilon)$, if positive, gives a measure of the power available to overcome frictional losses in the suction system.

11. Two methods are used to obtain values of C_ε for the condition $T_j = m_s U_0$. Method I, described in Appendix IV, allows values of $\varepsilon/m_s U_0^2$, and so of C_ε, to be determined from measured values of m_s and H_c, where H_c is the peak stagnation pressure in the jet of air flowing out of the slot. These values of C_ε take into account slot losses. Method II, described in Appendix V, is based on a theoretical relation derived for a boundary layer which has not separated from the surface upstream of the slot. This relation does not include slot losses nor the additional work to be done if the boundary layer separates from the surface upstream of the slot position. Shock wave losses at entry, estimated on the assumption that the shock wave is plane and normal to the aerofoil surface, are included. Curves of $\varepsilon/m_b u_1^2$ against m_s/m_b, calculated by Method II for a turbulent velocity profile $u/u_1 = (y/\delta)^{1/7}$ at the slot position, are given in Fig. 11. Curves for a laminar velocity profile are given in Fig. 12. These curves show how the value of $\varepsilon/m_b u_1^2$ depends on the form of the velocity profile and on the value of u_1 at the slot position.

12. Values of C_ε obtained by each method for Cases I–IV and the condition C_{Ds} a minimum are given in Table 1. Those by Method I are greater than those by Method II, the ratios for the four cases being 3·7, 1·5, 3·1 and 2·5 respectively. The values of C_ε given by Method I include losses in the slot, and they are pessimistic because the slot has a poor efficiency. In fact there is definite direct evidence (*see* Appendix IV), that separation occurs in the slot for Case III. On the other hand, the values by Method II are optimistic for they do not include slot losses, nor, for Case IV, any additional work associated with boundary-layer separation upstream of the slot.

13. Table 1 shows that all the values of $(C_D - C_{Ds} - C_\varepsilon)$ obtained by Method I are negative. Excluding Case III, because C_ε is doubtful (*see* Appendix VI), they are $-0{\cdot}0033$, $-0{\cdot}0012$ and $-0{\cdot}0035$, that is, − 31 per cent, − 6 per cent. and − 10 per cent. of the corresponding values of C_D, the drag coefficient without suction. The values obtained by Method II are positive for Cases I, II and IV and negative for Case III. They are $+0{\cdot}0020$, $+0{\cdot}0014$, $+0{\cdot}0112$ and $-0{\cdot}0003$ respectively, that is, + 21 per cent., + 7 per cent. (+ 16 per cent. if layer is laminar), 32 per cent. and − 2 per cent. of the corresponding values of C_D.

The conclusion to be drawn for Cases II, $M = 0{\cdot}735$, $\alpha = 0$ deg. and IV $M = 0{\cdot}730$, $\alpha = 4$ deg., is that $C_D - C_{Ds} \doteqdot C_\varepsilon$. In other words, the power saved by the reduction in drag due to suction is about the same as the estimated compressor power. Case III is one for which the boundary layer is separating near the slot position, and the results obtained by Method I are not satisfactory, because of flow separation within the slot and the related uncertainty in the estimated value of C_ε. Case IV is the most interesting one because it deals with suction behind a shock wave which has caused the boundary layer to separate from the surface.

TABLE 1

Values of $(C_D - C_{Ds} - C_\varepsilon)$ *for the Condition* C_{Ds} *a Minimum*
Single Slot in Upper Surface (B)

Case	$\alpha°$	M	C_D	C_{Ds} (min.)	$\frac{m_s 10^3}{\rho_0 U_0 c}$ for minimum C_{Ds}	Method I			Method II				
						$\frac{\varepsilon}{m_s U_0^2}$ (Table 4)	C_ε	$(C_D - C_{Ds} - C_\varepsilon)$	$\frac{u_1}{U_0}$ at $x = 0{\cdot}5c$	$\frac{m_s}{m_b}$ (Approx.)	$\frac{\varepsilon}{m_s u_1^2}$	C_ε	$(C_D - C_{Ds} - C_\varepsilon)$
I	0	0·630	0·0107	0·0065	6·1	0·62	0·0075	−0·0033	1·44	1·40(*a*)	0·079	0·0020	0·0022
II	0	0·725	0·0202 0·0186	0·0134† 0·0122	3·2	1·22	0·0078	−0·0010† −0·0014	1·74	0·30(*b*) [0·75]	0·270 [0·179]	0·0052 [0·0035]	0·0016† 0·0012 [0·0031]
III	4	0·681	0·0189	0·0104	7·7	1·78*	0·0274*	−0·0199	1·80	0·67(*c*)	0·177	0·0088	−0·0003
IV	4	0·730	0·0345	0·0135	5·5	2·23	0·0245	−0·0035	1·95	0·52(*c*)	0·235	0·0098	0·0112

* Doubtful values.
† Under surface (A).
(*a*) Boundary layer laminar.
(*b*) Boundary layer assumed to be turbulent. The values in square brackets are for a laminar layer.
(*c*) Boundary layer turbulent.

14. *Conclusion.*—It must be emphasised that the experiments were made at low Reynolds numbers on a thick conventional aerofoil section and that no attempt was made to design an efficient slot, nor to obtain the most effective position of the slot. In view of these shortcomings it is not possible to assess from the experimental results the gain in performance to be expected from boundary-layer suction under the more favourable conditions associated with the higher Reynolds numbers of flight, but the fact that $C_D - C_{D_s} \doteqdot C_\varepsilon$ for the unfavourable conditions of the experiments gives promise that, at the Reynolds numbers of flight and for an efficient slot and suction system, the drag coefficient at the critical Mach number can be maintained to a higher Mach number, say 0·1 higher, by boundary-layer suction with an economic use of power. An estimation of the gain to be expected at the higher Reynolds number of flight can be obtained from the fact that for a given value of m_s/m_b, $C_\varepsilon \propto (U_0 c/\nu)^{-0\cdot2}$, for a turbulent boundary layer, and $C_\varepsilon \propto (U_0 c/\nu)^{-0\cdot5}$ for a laminar boundary layer. For the present experiments, $U_0 c/\nu \doteqdot 6\cdot8 \times 10^5$.

APPENDIX I

Suction System

Fig. 2 gives a diagrammatic sketch of the suction system. The air sucked through the aerofoil slot flows through a small chamber (*a*), capacity 0·9 cubic ft., a plate orifice (*b*), a control valve (*c*) and a large suction chamber (*d*), capacity 90 cubic ft. The pressure in chamber (*d*) was maintained at about 5 in. mercury abs. For this pressure, the valve behaved as a choke and consequently the flow upstream of the valve was not affected by pressure fluctuations in chamber (*d*). Details of the control valve are given at the bottom of Fig. 2.

A $\frac{1}{2}$ in. Hodgson plate orifice in a 1 in. pipe was used to measure the rate at which air was sucked. It can be shown, from relations given in Ref. 8, that for these dimensions the rate of flow is given by

$$M = 0\cdot00192\left[1 + 0\cdot43\frac{p_2}{p_1}\right]\sqrt{\{\rho_1(h_1 - h_2)\}},$$

where M is the mass in slugs per sec., p_2/p_1 is the ratio of the pressure on the downstream side of the orifice plate to that on the upstream side, ρ_1 is the air density, slugs per cubic foot, in the pipe upstream of the plate, and $(h_1 - h_2)$ is the pressure difference at the orifice plate, measured in inches of water. For the delivery rates of experiment, ρ_1 can be taken to be the same as that in the pressure chamber (*a*). Hence $\rho_1 = 0\cdot0228p/(273 + t)$, where p is the pressure in inches of mercury and t is the temperature in deg. *C.*, measured in the chamber.

APPENDIX II

Theoretical values of $m_b/\rho_0 U_0 c$ and δ/c at the Slot Position

1. Values of $m_b/\rho_0 U_0 c$ and δ/c at the slot position for a boundary layer which has not separated from the aerofoil surface have been calculated for values of θ obtained from a solution of boundary-ayer equations for compressible flow by the Young-Winterbottom method given in Ref. 9.

The relation for the momentum thickness, θ, at the slot position is obtained for a laminar boundary layer from a graphical solution of the equation

$$\left(\frac{\mathscr{R}\,\theta}{\rho_0\ c}\right)^2 \frac{U_0 c}{\nu_0} = \frac{0\cdot470\ (1 - 0\cdot142M^2)\ (\mu_W/\mu_0)}{(u_1/U_0)^n} \int_0^{0\cdot5} \left(\frac{u_1}{U_0}\right)^{n-1} \frac{\mathscr{R}}{\rho_0}\, d\left(\frac{s}{c}\right)$$

where $n = 6\cdot28\ (1 + 0\cdot152M^2)$

and $\mu_W/\mu_0 = 1 + 0\cdot164M^2$.

At the stagnation point $(u_1'/\mu_W\mathscr{R})\ (\mathscr{R}\theta)^2 = 0\cdot0748\ (1 - 0\cdot294M^2)$.

2. The value of θ at the slot position is obtained for a turbulent boundary layer by a step-by-step integration of the equation

$$\frac{d\zeta}{ds} + \frac{6{\cdot}13}{u_1}\frac{du_1}{ds} = \frac{u_1 \mathscr{R}}{\mu_W} F(\zeta),$$

where $\zeta^2 = \mathscr{R} u_1^2/\tau$,

τ = intensity of surface friction,

$F(\zeta) = 10{\cdot}411\ \zeta^{-2} e^{-0{\cdot}3914\zeta}$,

and $\zeta = 5{\cdot}882 \log_{10}\{4{\cdot}075\ (u_1 \mathscr{R}\theta/\mu_W)$.

Values of $F(\zeta)$ are tabulated in Ref. 10. The value of $\mathscr{R}\theta$ at a transition point is taken to be that obtained from the solution of the laminar boundary layer equations for the flow forward of the transition point.

3. In view of the fact that direct measurement of the values of $m_b/\rho_0 U_0 c$ and δ/c at the slot position was not possible, because of the small size of the models, it was decided to obtain an idea of the magnitude of these quantities from calculations made for the distributions of u_1/U_0 measured for the values of $m_s/\rho_0 U_0 c$ for which C_{Ds} is a minimum, for two assumed types of flow, (i) a laminar boundary layer and (ii) a layer laminar to $0{\cdot}18c$ and turbulent beyond. The values of θ for these conditions were obtained from the relations given above. Further, it was assumed for the laminar layer that the velocity profile at the slot position was the same as the Blasius profile for incompressible flow, $\Lambda = 0$, and for the turbulent layer that the profile was given by $u/u_1 = (y/\delta)^{1/7}$. The value of $m_b/\rho_0 U_0 c$ is given by $\frac{\mathscr{R}}{\rho_0}\frac{u_1}{U_0}\frac{\delta}{c}\left(1 - \frac{\delta^*}{\delta}\right)$, where δ^* is the displacement thickness given by $\int_0^\delta \left(1 - \frac{\rho}{\mathscr{R}}\frac{u}{u_1}\right) dy$.

TABLE 2

Results of boundary-layer calculations

(i) Conditions for which curves of u_1/U_0 were obtained

Case	α°	M	$\frac{U_0 c}{\nu} \times 10^{-5}$	C_{Ds} (min.)	$\frac{m_s\ 10^3}{\rho_0 U_0 c}$ for C_{Ds} (min.)	$\frac{u_1}{U_0}$ at $x = 0{\cdot}5c$	$\frac{\mathscr{R}}{\rho_0}$ at $x = 0{\cdot}5c$	
I	0	0·630	6·27	0·0065	6·1	1·420	0·810	
II	0	0·735	6·98	0·0134 (A) 0·0122 (B)	3·2	1·605	0·632	(A) slot on surface A. (B) slot on surface B.
III	4	0·681	6·62	0·0104	7·7	1·735	0·597	
IV	4	0·730	6·93	0·0135	5·5	1·730	0·546	

(ii) Values at slot position

Conditions	Case	u_1 f.p.s.	$\frac{\delta^*}{\delta}$	$\frac{\theta}{\delta}$	$\frac{\delta\ 10^3}{c}$	$\frac{m_b\ 10^3}{\rho_0 U_0 c}$	$\frac{m_s \text{ for } C_{Ds} \text{ min.}}{m_b}$
Boundary layer laminar* Blasius distribution of u/u_1 for $\Lambda \doteqdot 0$ at $x = 0{\cdot}5c$. No separation in front of slot.	I	960	0·286	0·0923	5·3	4·4	1·40
	II	1,248	0·308	0·0842	6·0	4·4	0·75
	III	1,260	0·309	0·0840	6·6	4·7	1·65
	IV	1,335	0·316	0·0814	7·2	4·7	1·15
Boundary layer turbulent from $x = 0{\cdot}18c$ to $x = 0{\cdot}5c$.† $u/u_1 = (y/\delta)^{1/7}$ at $x = 0{\cdot}5c$. No separation in front of slot.	I	960	0·150	0·0972	10·7	10·4	0·59
	II	1,248	0·182	0·0870	13·0	10·8	0·30
	III	1,260	0·183	0·0865	13·6	11·5	0·67
	IV	1,335	0·191	0·0847	13·8	10·6	0·52

* Boundary layer is likely to be laminar for Case I and possibly for Case II.

† The layer is likely to be turbulent for Cases III and IV.

TABLE 3

	α°	M	$\frac{U_0 c}{\nu_0} 10^{-5}$	$\frac{u_1}{U_0}$	$\frac{\mathscr{R}}{\rho_0}$	$\frac{\delta^*}{\delta}$	$\frac{\theta}{\delta}$	$\frac{\delta}{c}\left(\frac{U_0 c}{\nu}\right)^{\frac{1}{2}}$	$\frac{m_b 10^3}{\rho_0 U_0 c}$
Theoretical distribution of u_1/U_0 for compressible flow, $m_s = 0$.	0	0·63	6·27	1·250	0·892	0·280	0·0948	7·2	6·5
Theoretical distribution of u_1/U_0 for incompressible flow, $m_s = 0$.	0	—	6·27	1·178	1	0·262	0·100	5·3	5·8

4. The results of the calculations are given in Table 2. For each velocity profile, δ^*/δ increases and θ/δ decreases with u_1. The values of δ/c and of $m_b/\rho_0 U_0 c$ for the laminar velocity profile are about one-half of those for the turbulent velocity profile $u/u_1 = (y/\delta)^{1/7}$.

Table 3 gives results which are not strictly relevant to the present analysis but they are included because they show that the value of $m_b/\rho_0 U_0 c$ calculated for a laminar boundary layer and the theoretical distribution of u_1/U_0 for compressible flow, $M = 0{\cdot}63$, differs by only 12 per cent. from that for incompressible flow. This result is consistent with that obtained from a similar comparison given in Ref. 9. The theoretical distribution of u_1/U_0 for incompressible flow was taken from Ref. 6. The distribution of u_1/U_0 for compressible flow was obtained from that for the incompressible flow by the Temple-Yarwood relations given in Ref. 7. The calculations are made on the assumption that boundary layer separation does not occur in front of the slot, and that for both compressible and incompressible flows the velocity profile at the slot position is the same as the Blasius profile, $\Lambda = 0$, for incompressible flow.

APPENDIX III

Economy of Boundary-layer Suction
Two-dimensional Subsonic Compressible Flow

It can be shown, by the method given in Ref. 4, for two-dimensional subsonic compressible flow past an aerofoil with a spanwise slot that when the air sucked into the aerofoil is discharged in the direction of its span the drag per unit span is

$$\int(p_0 - p)\,dy + \int \rho u\,(U_0 - u)\,dy + m_s U_0\,,$$

where p and ρ are the static pressure and density of the air at any point, p_0 and U_0 are the static pressure and velocity in the undisturbed stream, u is the component of the velocity at any point parallel to the undisturbed flow, m_s is the mass of air sucked into the aerofoil per sec. per unit span, y is the lateral distance across the wake, and the integrals are taken along a straight line cutting the wake at right-angles to the undisturbed stream. This relation holds when limited shock waves are present. The sum of the first two terms when the integrals are confined to the wake and taken at a section where the pressure is p_0 becomes $\int \rho u(U_0 - u)\,dy$. The relation used for estimating the profile drag per unit span by the pitot-traverse method is derived from this integral.

The total drag is therefore $D_s + m_s U_0$, where D_s is the drag measured by the pitot-traverse method.† This relation holds for an aerofoil mounted between tunnel walls, the air sucked into the aerofoil being discharged outside the tunnel, as in the present experiments, provided the

† The drag per unit span of a transverse line-sink in two-dimensional flow of a perfect fluid between parallel planes is $m_s\,(U_0 + U_1)/2$, where m_s is the strength of the sink per unit span, U_0 and U_1 are the velocities far upstream and far downstream respectively and the image effect due to the walls is ignored. The value of $\int(p_0 - p)\,dy + \int \rho u\,(U_0 - u)\,dy$ is $-\,m_s\,U_0\,(m_s/2\rho h U_0)$, where h is the distance between the walls. The sum of these integrals therefore becomes small compared with $m_s\,U_0$ when $m_s/\rho h U_0$ is small. The drag obtained by the pitot-traverse method for an aerofoil in a wind-tunnel stream is therefore that associated with the frictional losses in the wake provided, as in the present experiments, that $m_s/\rho h U_0$ is small.

velocity due to the sink is negligibly small at the point where the datum velocity is measured. When the air sucked into the aerofoil is discharged in the backward direction the power per unit span needed to drive the aerofoil through the air with a velocity U_0 is $U_0/\eta \cdot (D_s + m_s U_0 - T_j)$, where η is the efficiency of the main propulsive system and T_j is the thrust per unit span due to the jet reaction.

The power, P, absorbed by the compressor is $1/\eta_1 \cdot (\varepsilon + \varepsilon_f)$ per unit span, where η_1 is the compressor efficiency, ε is the work per second per unit span to raise the velocity and pressure of the sucked air to those in the jet exit, and ε_f is the work done per second per unit span against the frictional resistance of the duct system, excluding that of the compressor.

The total power is therefore

$$\frac{U_0}{\eta}[D_s + m_s U_0 - T_j] + \frac{1}{\eta_1}[\varepsilon + \varepsilon_f],$$

and the effective drag, D_1, is

$$[D_s + m_s U_0 - T_j] + \frac{\eta}{\eta_1 U_0}[\varepsilon + \varepsilon_f].$$

The difference $D - D_1$, where D is the drag per unit span of the aerofoil without suction, is the effective gain in drag due to suction.

For the present analysis we take $T_j = m_s U_0$ and $\eta/\eta_1 = 1$. Suction has a beneficial effect, therefore, if $\left(D_s + \frac{\varepsilon}{U_0} + \frac{\varepsilon_f}{U_0}\right) < D$, that is, if $\left(D - D_s - \frac{\varepsilon}{U_0}\right) > \frac{\varepsilon_f}{U_0}$. Dividing by $\frac{1}{2}\rho_0 c U_0^2$ this relation becomes $(C_D - C_{Ds} - C_\varepsilon) > C\varepsilon_f$ where $C_D = \frac{2D}{\rho_0 c U_0^2}$, $C_{Ds} = \frac{2D_s}{\rho_0 c U_0^2}$, $C_\varepsilon = \frac{2\varepsilon}{\rho_0 c U_0^3}$, and $C\varepsilon_f = \frac{2\varepsilon_f}{\rho_0 c U_0^3}$.

APPENDIX IV

Estimation of $\varepsilon/m_s U_0^2$ from Measured Values of m_s and H_c for the Condition $T_j = m_s U_0$

1. The condition $T_j = m_s U_0$ is satisfied when the air sucked into the aerofoil is compressed adiabatically and discharged backwards with the velocity U_0 and the pressure p_0 of the undisturbed stream. An estimate of the work, ε, done per second per unit span to compress the air adiabatically can be obtained from measurements of m_s and the peak stagnation pressure H_c provided certain assumptions are made. Those made in the present analysis are :—

(i) the flow in the slot is axial and two-dimensional,

(ii) the stagnation temperature, T_H, of the air in the slot is constant and equal to that in the undisturbed stream, *i.e.*, the total energy per unit mass is constant and equal to $\left(\frac{\gamma}{\gamma - 1}\frac{p_0}{\rho_0} + \frac{U_0^2}{2}\right)$,

(iii) the static pressure, p_3, is constant across a section of the slot,

(iv) the stagnation pressure, H_3, within the slot falls linearly from a peak value H_c on the centre-line to p_3 at the slot walls,

(v) the peak stagnation pressure in the slot at the section taken is equal to that measured in the jet issuing from the slot into the aerofoil, and

(vi) the static pressure, p_3, taken is that for which the calculated and measured values of m_s are the same.

It was found that the value of $\varepsilon/m_s U_0^2$ was not very sensitive to the form taken for the fall in H_3 from the peak value H_c, and that the assumption of a linear fall is not inconsistent with that given by measurements taken in the jet flowing out of the slot, see below.

On the above assumptions we have

$$\frac{H_3}{\rho_H} = \frac{p_A}{\rho_A}, \text{ since } T_H = T_A \quad .. \quad .. \quad .. \quad .. \quad .. \quad .. \quad .. \quad (1)$$

$$\frac{p_3}{\rho_3^\gamma} = \frac{H_3}{\rho_H^\gamma}. \quad .. \quad .. \quad .. \quad .. \quad .. \quad .. \quad .. \quad .. \quad (2)$$

Hence,

$$\frac{\rho_3}{\rho_A} = \frac{\rho_H}{\rho_A}\left(\frac{H_3}{p_3}\right)^{-1/\gamma} = \frac{p_3}{p_A}\left(\frac{H_3}{p_3}\right)^{(\gamma-1)/\gamma} \quad .. \quad .. \quad .. \quad .. \quad .. \quad (3)$$

where H_3 and ρ_H are the stagnation pressure and density in the slot, ρ_3 is the density of the air in the slot, and p_A and ρ_A are the atmospheric pressure and density. Further, if u_3 is the velocity in the slot, we have

$$\tfrac{1}{2}\rho_3 u_3^2 = \frac{\gamma}{\gamma-1} p_3 \left\{\left(\frac{H_3}{p_3}\right)^{(\gamma-1)/\gamma} - 1\right\}, \quad .. \quad .. \quad .. \quad .. \quad .. \quad (4)$$

and

$$\left(\frac{u_3}{a_A}\right)^2 = \frac{2}{\gamma-1}\frac{p_3}{p_A}\frac{\rho_A}{\rho_3}\left\{\left(\frac{H_3}{p_3}\right)^{(\gamma-1)/\gamma} - 1\right\} = \frac{2}{\gamma-1}\left\{1 - \left(\frac{p_3}{H_3}\right)^{(\gamma-1)/\gamma}\right\} \quad .. \quad (5)$$

where a_A is the atmospheric velocity of sound.

The work done on the air to increase its pressure to p_0 and its velocity to U_0 is equal to the increase of total energy.

Hence

$$\varepsilon = t\int_{-1/2}^{1/2}\left[\left(\frac{\gamma}{\gamma-1}\frac{p_0}{\rho_4} + \frac{U_0^2}{2}\right) - \left(\frac{\gamma}{\gamma-1}\frac{p_0}{\rho_0} + \frac{U_0^2}{2}\right)\right]\rho_3 u_3 d\left(\frac{y}{t}\right)$$

$$= \frac{t\gamma}{\gamma-1}\frac{p_0}{\rho_0}\int_{-1/2}^{1/2}\left(\frac{\rho_0}{\rho_4} - 1\right)\rho_3 u_3 d\left(\frac{y}{t}\right),$$

where ρ_4 is the density in the discharged jet.

Now $\dfrac{p_3}{\rho_3^\gamma} = \dfrac{p_0}{\rho_4^\gamma}$. Hence $\left(\dfrac{\rho_0}{\rho_4} - 1\right) = \left[\dfrac{\rho_0}{\rho_3}\left(\dfrac{p_3}{p_0}\right)^{1/\gamma} - 1\right]$; and

$$\varepsilon = \frac{t\gamma}{\gamma-1}\frac{p_0}{\rho_0}\int_{-1/2}^{1/2}\left[\frac{\rho_0}{\rho_3}\left(\frac{p_3}{p_0}\right)^{1/\gamma} - 1\right]\rho_3 u_3 d\left(\frac{y}{t}\right)$$

$$= \frac{ta_0^2}{\gamma-1}\rho_A a_A \int_{-1/2}^{1/2}\left[\frac{\rho_0}{\rho_3}\left(\frac{p_3}{p_0}\right)^{1/\gamma} - 1\right]\frac{\rho_3}{\rho_A}\frac{u_3}{a_A} d\left(\frac{y}{t}\right),$$

since $a_0^2 = \dfrac{\gamma p_0}{\rho_0}$.

Further,

$$m_s = ta_A\rho_A\int_{-1/2}^{1/2}\frac{\rho_3}{\rho_A}\frac{u_3}{a_A} d\left(\frac{y}{t}\right), \quad .. \quad .. \quad .. \quad .. \quad .. \quad .. \quad (6)$$

so that

$$\frac{\varepsilon}{m_s U_0^2} = \frac{\displaystyle\int_{-1/2}^{1/2}\left[\frac{\rho_0}{\rho_3}\left(\frac{p_3}{p_0}\right)^{1/\gamma} - 1\right]\frac{\rho_3}{\rho_A}\frac{u_3}{a_A} d\left(\frac{y}{t}\right)}{(\gamma-1)M^2\displaystyle\int_{-1/2}^{1/2}\frac{\rho_3}{\rho_A}\frac{u_3}{a_A} d\left(\frac{y}{t}\right)}. \quad .. \quad .. \quad .. \quad .. \quad (7)$$

2. The peak stagnation pressure, H_c, of the air flowing through the slot was determined from a pitot traverse made across the jet inside the aerofoil, close behind the slot exit. The tube axis was parallel to the slot axis, *i.e.* at 45 deg. to the inner surface of the aerofoil wall, Fig. 1. The external width of the tube mouth was 0·02 in., *i.e.* $0{\cdot}6t$, and the breadth was 0·06 in., *i.e.* $1{\cdot}7t$, where t is the width of the slot measured normal to its centre-line. The tube was mounted near the end of a bar carried within the aerofoil on a pivot 2-in. above the tube. The lateral position of the tube was given by a micrometer reading of the position of the end of the bar outside the tunnel.

The pitot-traverse curves had well-defined peaks, provided the mass of air sucked was not too small. The stagnation pressure fell linearly with the lateral distance from the peak value, except near the boundaries, beyond which the pressure became constant. The pressure diagrams were about 70 per cent. wider than the width of the slot, $t\sqrt{2}$, in the direction of the pitot traverse. The readings near the jet boundaries are suspect because they include unknown effects due to wall interference, the relatively large width of the pitot tube and to deviations from an axial direction of flow. The measured peak stagnation pressures should, however, be reasonably reliable.

3. Values of $\varepsilon/m_s U_0^2$ calculated, on the assumptions made in § 1, from relation (7) for measured values of $m_s/\rho_0 U_0 c$ and H_c/p_A (one slot) are given in Table 4. For Cases I, II and IV, the calculations were made for two values of $m_s/\rho_0 U_0 c$. The two values of $\varepsilon/m_s U_0^2$ obtained do not differ much, and mean values can be taken for the condition C_{Ds} a minimum. The value of $\varepsilon/m_s U_0^2$ for Case III is doubtful, for it would appear from the narrower width of the stagnation-pressure diagram, compared with those for the other cases, and also from the difference in the shape of the diagram, that flow separation occurs within the slot. The assumptions made in the calculations do not therefore hold.

TABLE 4

Case	$\alpha°$	M	Measured		Calculated		Value of $\frac{m_s 10^3}{\rho_0 U_0 c}$ at $(C_{Ds})_{min.}$
			$\frac{m_s 10^3}{\rho_0 U_0 c}$	$\frac{H_c}{p_A}$	$\frac{p_3}{p_A}$	$\frac{\varepsilon}{m_s U_0^2}$	
I	0	0·630	4·1 8·0	0·686 0·845	0·657 0·568	0·63 0·61 } 0·62	6·1
II	0	0·735	3·8 3·0	0·429 0·409	0·385 0·384	1·12 1·32 } 1·22	3·2
III	4	0·681	5·6	0·424	0·270	1·78	7·7
IV	4	0·730	4·3 3·0	0·289 0·289	0·189 0·230	2·31 2·15 } 2·23	5·5

APPENDIX V

A Theoretical Relation for $\varepsilon/m_s u_1^2$ for the Condition $T_j = m_s U_0$, Applicable to a Boundary Layer which has not Separated from the Aerofoil Surface

1. The boundary-layer forward of a slot is either in contact with or separated from the aerofoil surface. When the boundary layer is in contact with the surface, the air sucked into the slot comes from the inner part of the layer provided $m_s < m_b$: when the layer is separated, the air comes from the " dead air " region between the separated layer and the surface and, if sufficient air is sucked, from the inner part of the initially separated layer. A relation for $\varepsilon/m_s u_1^2$ which does not take into consideration losses in the slot is derived below for a boundary layer in contact with the surface up to the slot position.

2. The velocity in the outer part of the layer sucked into the slot may exceed the local velocity of sound and a shock wave is then formed at the mouth of the slot. It is assumed that this shock wave is plane and normal to the aerofoil surface. The pressure, p, in the boundary layer just in front of the shock wave is taken to be constant and equal to the pressure, p_1, just outside the layer.

The condition of constant total energy per unit mass gives

$$\frac{\gamma}{\gamma-1}\frac{p_0}{\rho_0}+\frac{U_0^2}{2}=\frac{\gamma}{\gamma-1}\frac{p_1}{\rho}+\frac{u^2}{2}=\frac{\gamma}{\gamma-1}\frac{p_1}{\mathscr{R}}+\frac{u_1^2}{2}=\frac{\gamma}{\gamma-1}\frac{p_2}{\rho_2}+\frac{u_2^2}{2}, \quad \ldots \quad (1)$$

where ρ and u are the density and velocity in the boundary layer, $\mathscr{R}$ and u_1 are the density and velocity just outside the layer and p_2, ρ_2 and u_2 are the pressure, density and velocity immediately behind the shock wave at the slot entry.

For $u > a$, the local velocity of sound,

$$\frac{p_2}{p_1}=\frac{2\gamma}{\gamma+1}\cdot\frac{u^2}{a^2}-\frac{(\gamma-1)}{(\gamma+1)}, \text{ where } a^2=\frac{\gamma p_1}{\rho}, \quad \ldots \quad (2)$$

and

$$\frac{\rho_2}{\rho}=\frac{(\gamma+1)\frac{p_2}{p_1}+(\gamma-1)}{(\gamma-1)\frac{p_2}{p_1}+(\gamma+1)}. \quad \ldots \quad (3)$$

For $u < a$, we write $u = u_2$, $\rho = \rho_2$, $p_1 = p_2$ where suffix 2 now denotes values just behind a plane passing through the shock wave and extended to the aerofoil surface.

In the same manner as in Appendix IV, we have

$$m_s = \delta\rho_A a_A \int_0^{Y/\delta} \frac{\rho}{\rho_A}\frac{u}{a_A}\, d\left(\frac{y}{\delta}\right) \quad \ldots \quad (4)$$

$$\varepsilon = \frac{\delta a_0^2}{(\gamma-1)}\rho_A a_A \int_0^{Y/\delta}\left(\frac{\rho_0}{\rho_4}-1\right)\frac{\rho}{\rho_A}\frac{u}{a_A}\, d\left(\frac{y}{\delta}\right)$$

$$= \frac{\delta a_0^2}{(\gamma-1)}\rho_A a_A \int_0^{Y/\delta}\left[\frac{\rho_0}{\rho_2}\left(\frac{p_2}{p_0}\right)^{1/\gamma}-1\right]\frac{\rho}{\rho_A}\frac{u}{a_A}\, d\left(\frac{y}{\delta}\right) \quad \ldots \quad (5)$$

and

$$\frac{\varepsilon}{m_s u_1^2}=\frac{\int_0^{Y/\delta}\left[\frac{\rho_0}{\rho_2}\left(\frac{p_2}{p_0}\right)^{1/\gamma}-1\right]\frac{\rho}{\rho_A}\frac{u}{a_A}\, d\left(\frac{y}{\delta}\right)}{(\gamma-1)\left(\frac{u_1}{a_0}\right)^2\int_0^{Y/\delta}\frac{\rho}{\rho_A}\frac{u}{a_A}\, d\left(\frac{y}{\delta}\right)}, \quad \ldots \quad (6)$$

where Y is the thickness of the layer sucked into the slot.

It is of interest to note that when a shock wave is not present, we have $p_1/\mathscr{R}^\gamma = p_0/\rho_0^\gamma$, $p_1/\rho^\gamma = p_0/\rho_4^\gamma$ and $\rho_0/\rho_4 = \mathscr{R}/\rho$. The relation for the work done can then be expressed in the simple form

$$\frac{\varepsilon}{m_s u_1^2} = \frac{\int_0^{Y/\delta} \left(1 - \frac{\rho}{\mathscr{R}}\right) \frac{u}{u_1} \, d\left(\frac{y}{\delta}\right)}{(\gamma - 1)\left(\frac{u_1}{a_0}\right)^2 \int_0^{Y/\delta} \frac{\rho}{\mathscr{R}} \frac{u}{u_1} \, d\left(\frac{y}{\delta}\right)} \quad \ldots \ldots \ldots \ldots \ldots \ldots \quad (7)$$

For standard atmospheric conditions outside the tunnel,

$$E_0 = \frac{(1117)^2}{\gamma - 1}, \text{ and since } \frac{\gamma}{\gamma - 1}\frac{p_1}{\mathscr{R}} = E_0 - \frac{u_1^2}{2} \text{ and } \frac{\gamma}{\gamma - 1}\frac{p_1}{\rho} = E_0 - \frac{u^2}{2}$$

$$\text{we have } \frac{\rho}{\mathscr{R}} = \frac{\left[1 - 0{\cdot}2\left(\frac{u_1}{1117}\right)^2\right]}{\left[1 - 0{\cdot}2\left(\frac{u}{1117}\right)^2\right]} \text{ for } \gamma = 1{\cdot}4.$$

The range of a_0 covered in the experiments is small, 1065 to 1095 f.p.s. and the mean value 1080 f.p.s. can be taken.

3. Curves of $\varepsilon/m_b u_1^2$ against m_s/m_b for a turbulent velocity profile $u/u_1 = (y/\delta)^{1/7}$ just forward of the shock wave at the entry to the slot and for $u_1 = 1{,}000$, 1,250 and 1,500 f.p.s. are given in Fig. 11. Curves for a laminar velocity profile, compressible flow, having the same form as that for the Blasius incompressible flow, $\Lambda \doteqdot 0$, are given in Fig. 12. For $m_s/m_b = 0{\cdot}4$, the values of $\varepsilon/m_b u_1^2$ for the laminar velocity profile are about 25 per cent. greater than those for the turbulent velocity profile : for $m_s/m_b = 1{\cdot}0$, the values of $\varepsilon/m_b u_1^2$ for the laminar velocity profile are about the same as those for the turbulent velocity profile.

The dotted curves of Fig. 12 were obtained by ignoring the shock wave losses at the slot entry. The difference between these curves and the full-line curves gives therefore a measure of the effect of the shock losses on the value of $\varepsilon/m_b u_1^2$.

REFERENCES

No.	*Author*	*Title, etc.*
1	Owen and Young	Note on the Drag Effect of Shock Waves. A.R.C. 5958. R.A.E. Rept. Aero. 1749. June, 1942. (Unpublished.)
2	Lock	The Ideal Drag due to a Shock Wave. A.R.C. 5852. June, 1942. (To be published.)
3	Bailey and Wood	The Development of a High Speed Induced Wind Tunnel of Rectangular Cross Section. R. & M. 1791. February, 1937.
4	Lock, Hilton and Goldstein	Determination of Profile Drag at High Speeds by a Pitot Traverse Method. R. & M. 1971. September, 1940.
5	Beavan and Manwell	Tables for Use in the Determination of Profile Drag at High Speeds by the Pitot Traverse Method. R. & M. 2233. September, 1941.
6	Allen	A Simplified Method for the Calculation of Aerofoil Pressure Distribution. N.A.C.A. Technical Note No. 708. May, 1939.
7	Temple and Yarwood	The Approximate Solution of the Hodograph Equations for Compressible Flow. A.R.C. 6107. R.A.E. Rept. S.M.E. 3201. June, 1942. (Unpublished.)
8	Ower	Measurement of Air Flow. Chapman and Hall, Ltd., 2nd Edn., 1932.
9	Young and Winterbottom	Note on the Effect of Compressibility on the Profile Drag of Aerofoils at Subsonic Mach Numbers in the Absence of Shock Waves. R. & M. 2400. May, 1940.
10	Squire and Young	The Calculation of the Profile Drag of Aerofoils. R. & M. 1838. November, 1937.
11	Fage and Falkner	An Experimental Determination of the Intensity of Friction on the Surface of an Aerofoil. R. & M. 1315. April, 1930.

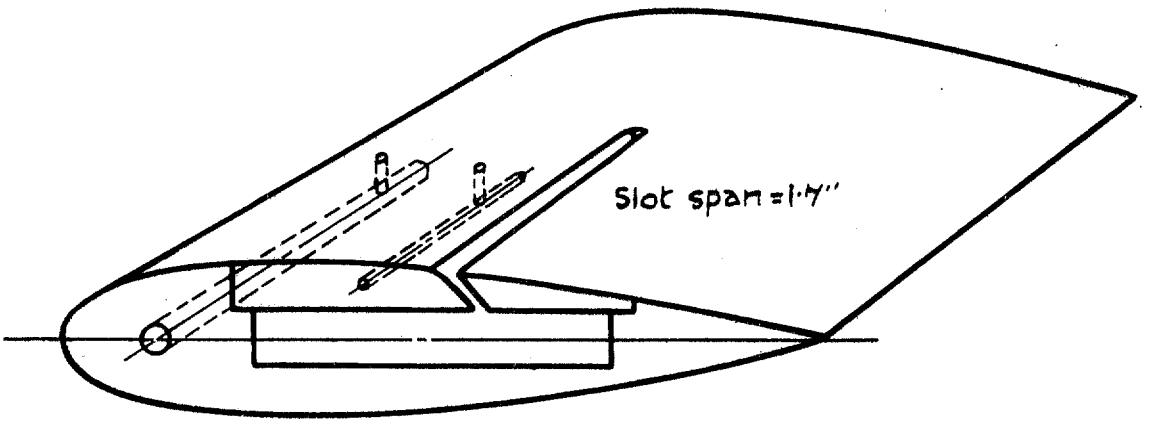

(*a*) Typical pressure hole systems, Model II.

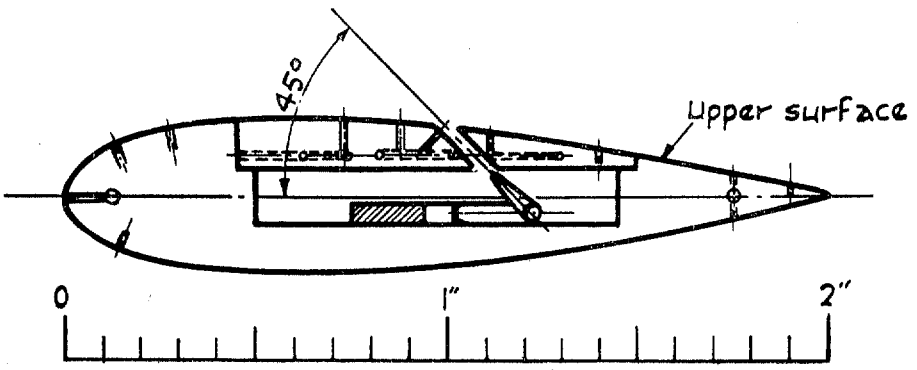

(*b*) Model II with pressure holes and traversing pitot tube.

FIG. 1.

Ordinates of Upper Surfaces of Models. (Median Section).

$\frac{x}{c}$	NACA 0020 $\frac{y}{c}$	Measured correction on true $\frac{y}{c}$		Actual $\frac{y}{c}$	
		Model I	Model II	Model I	Model II
0	0	0	0	0	0
0·025	0·0442	—	+0·0012	—	0·0454
0·027	0·0458	−0·0006	—	0·0452	—
0·091	0·0767	0	+0·0014	0·0767	0·0781
0·182	0·0946	−0·0002	−0·0012	0·0944	0·0934
0·273	0·0998	−0·0006	+0·0036	0·0992	0·1034
0·364	0·0989	−0·0004	+0·0070	0·0985	0·1059
0·455	0·0940	0	+0·0060	0·0940	0·1000
0·545	0·0854	0	+0·0048	0·0854	0·0902
0·636	0·0736	0	+0·0020	0·0736	0·0756
0·727	0·0590	0	+0·0010	0·0590	0·0600
0·818	0·0418	0	+0·0008	0·0418	0·0426
0·909	0·0227	+0·0008	0	0·0235	0·0227
1·000	0	0	0	0	0

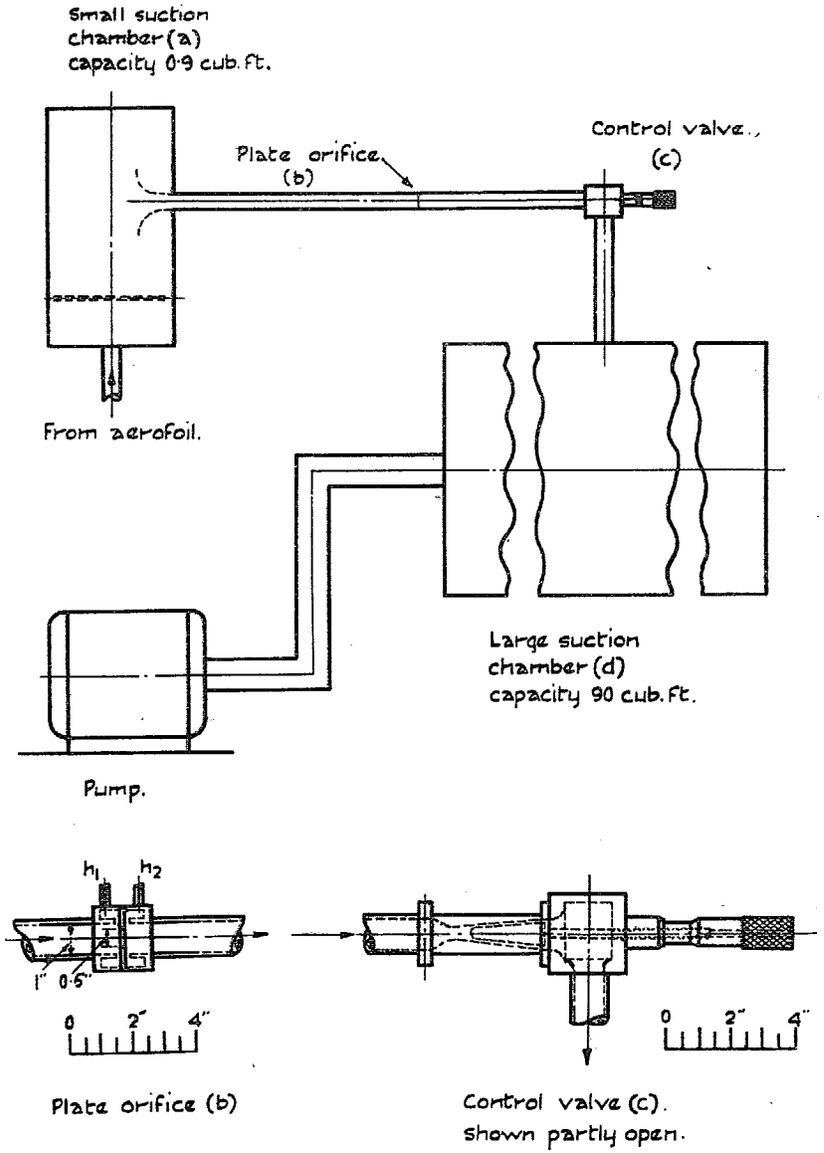

FIG. 2.

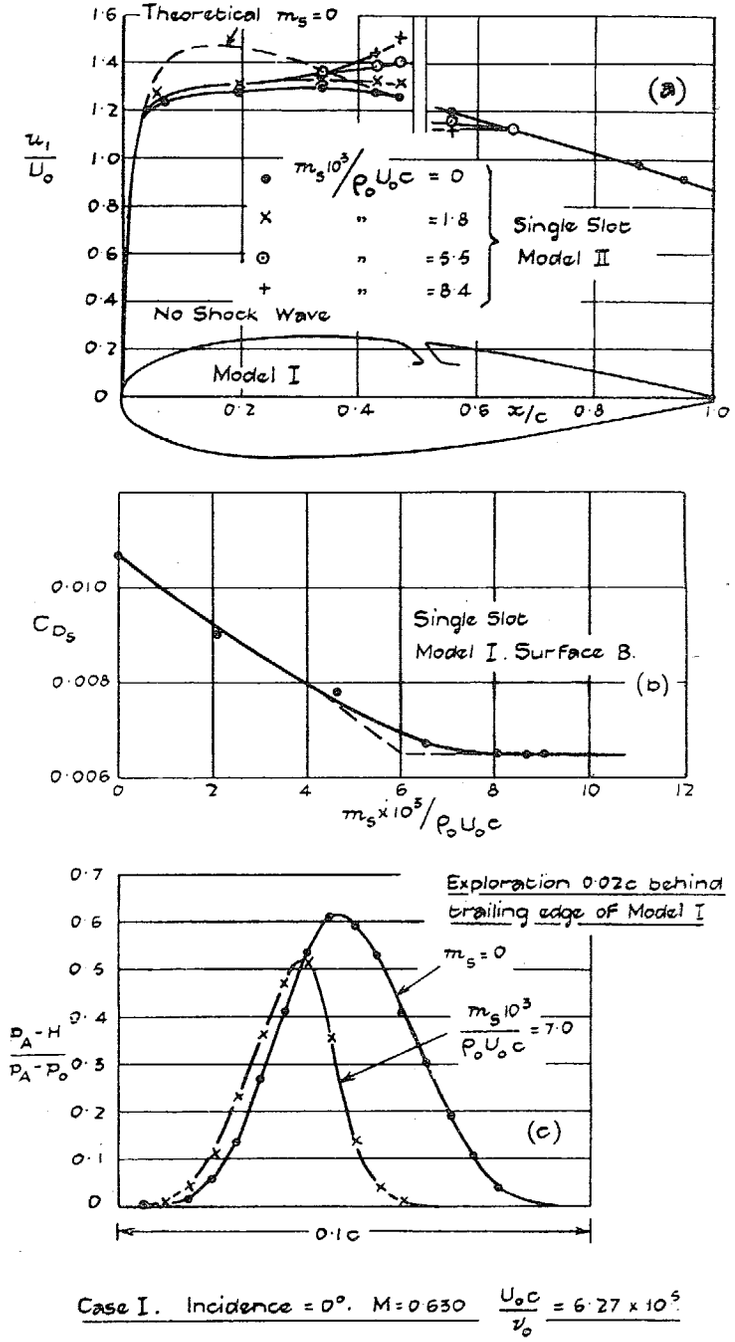

Case I. Incidence = 0°. M = 0·630 $\frac{U_0 c}{\nu_0} = 6{\cdot}27 \times 10^5$

FIG. 3.

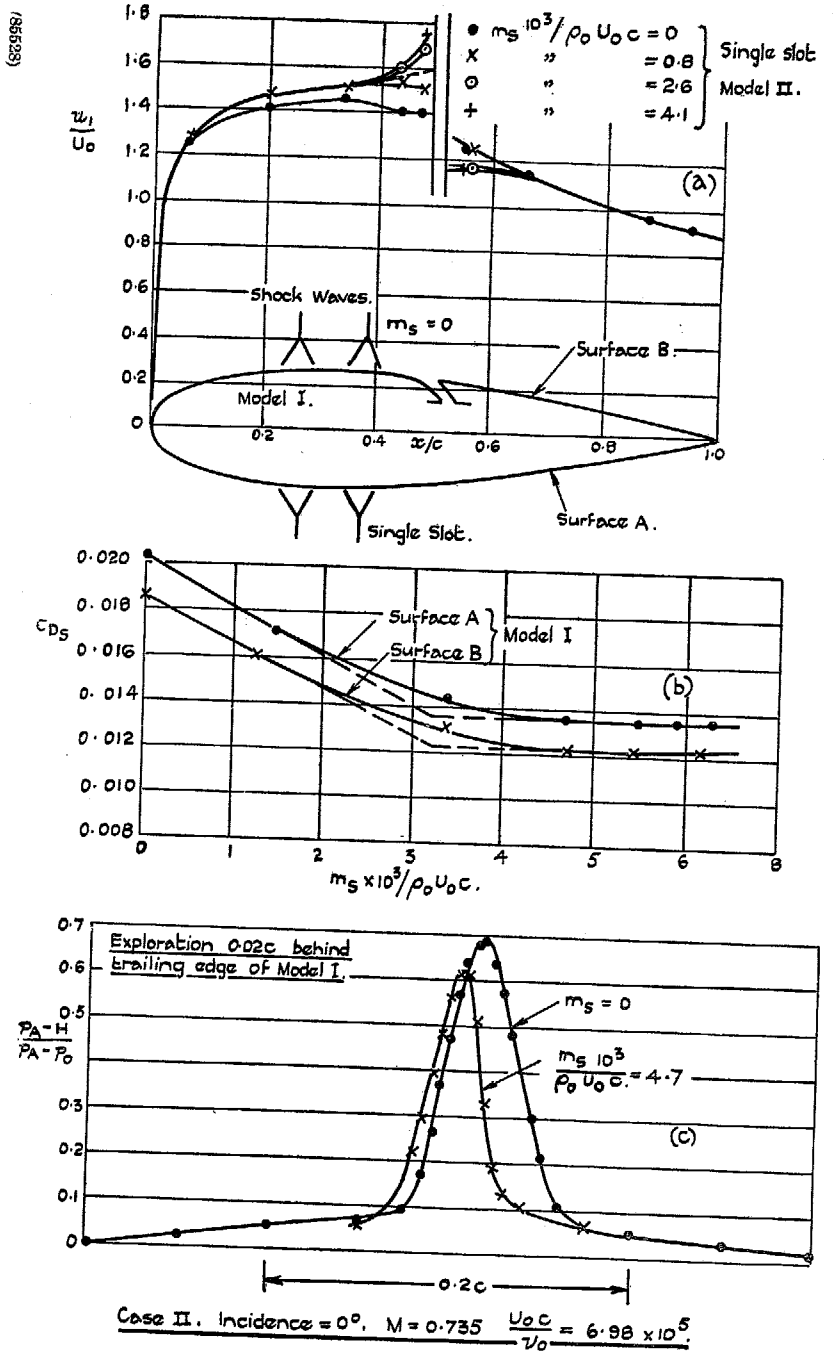
$m_s 10^3/\rho_0 U_0 c = 0$
$m_s 10^3/\rho_0 U_0 c = 0.8$
$m_s 10^3/\rho_0 U_0 c = 2.6$
$m_s 10^3/\rho_0 U_0 c = 4.1$
Single slot
Model II.
(a)
Shock Waves.
$m_s = 0$
Surface B.
Model I.
u_1/U_0
x/c
Single Slot.
Surface A.
C_{D_S}
Surface A
Surface B
Model I
(b)
$m_s \times 10^3/\rho_0 U_0 c$.
Exploration 0.02c behind trailing edge of Model I.
$m_s = 0$
$\frac{m_s 10^3}{\rho_0 U_0 c} = 4.7$
$\frac{p_A - H}{p_A - p_0}$
(c)
0.2c
Case II. Incidence = 0°, M = 0.735 $\frac{U_0 c}{\nu_0} = 6.98 \times 10^5$.

FIG. 4.

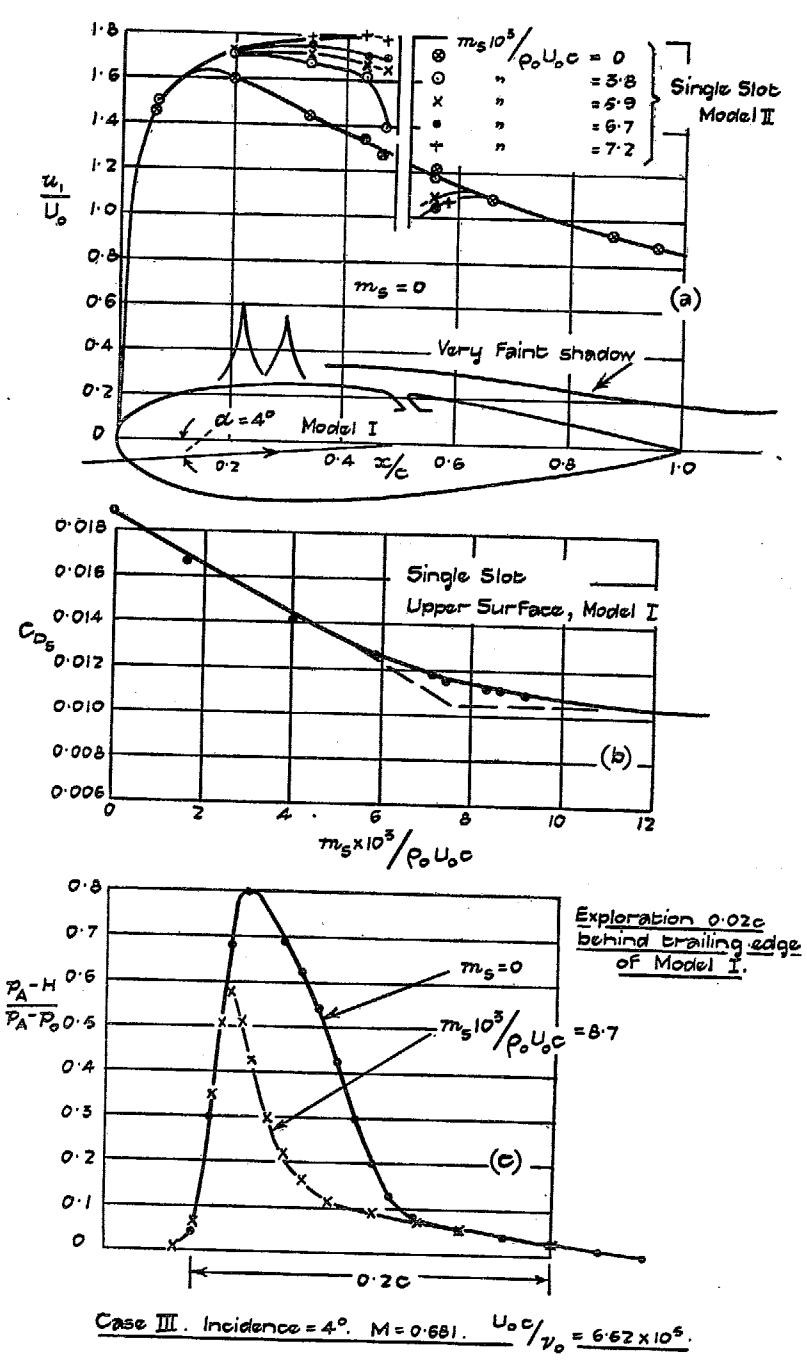
$m_s 10^3/\rho_0 U_0 c = 0$
$m_s 10^3/\rho_0 U_0 c = 3.8$
$m_s 10^3/\rho_0 U_0 c = 5.9$
$m_s 10^3/\rho_0 U_0 c = 6.7$
$m_s 10^3/\rho_0 U_0 c = 7.2$
Single Slot
Model II
u_1/U_0
$m_s = 0$
(a)
Very Faint shadow
$\alpha = 4°$
Model I
x/c
C_{D_S}
Single Slot
Upper Surface, Model I
(b)
$m_s \times 10^3/\rho_0 U_0 c$
Exploration 0.02c behind trailing edge of Model I.
$m_s = 0$
$m_s 10^3/\rho_0 U_0 c = 8.7$
$\frac{p_A - H}{p_A - p_0}$
(c)
0.2c
Case III. Incidence = 4°. M = 0.681. $U_0 c/\nu_0 = 6.62 \times 10^5$.

FIG. 5.

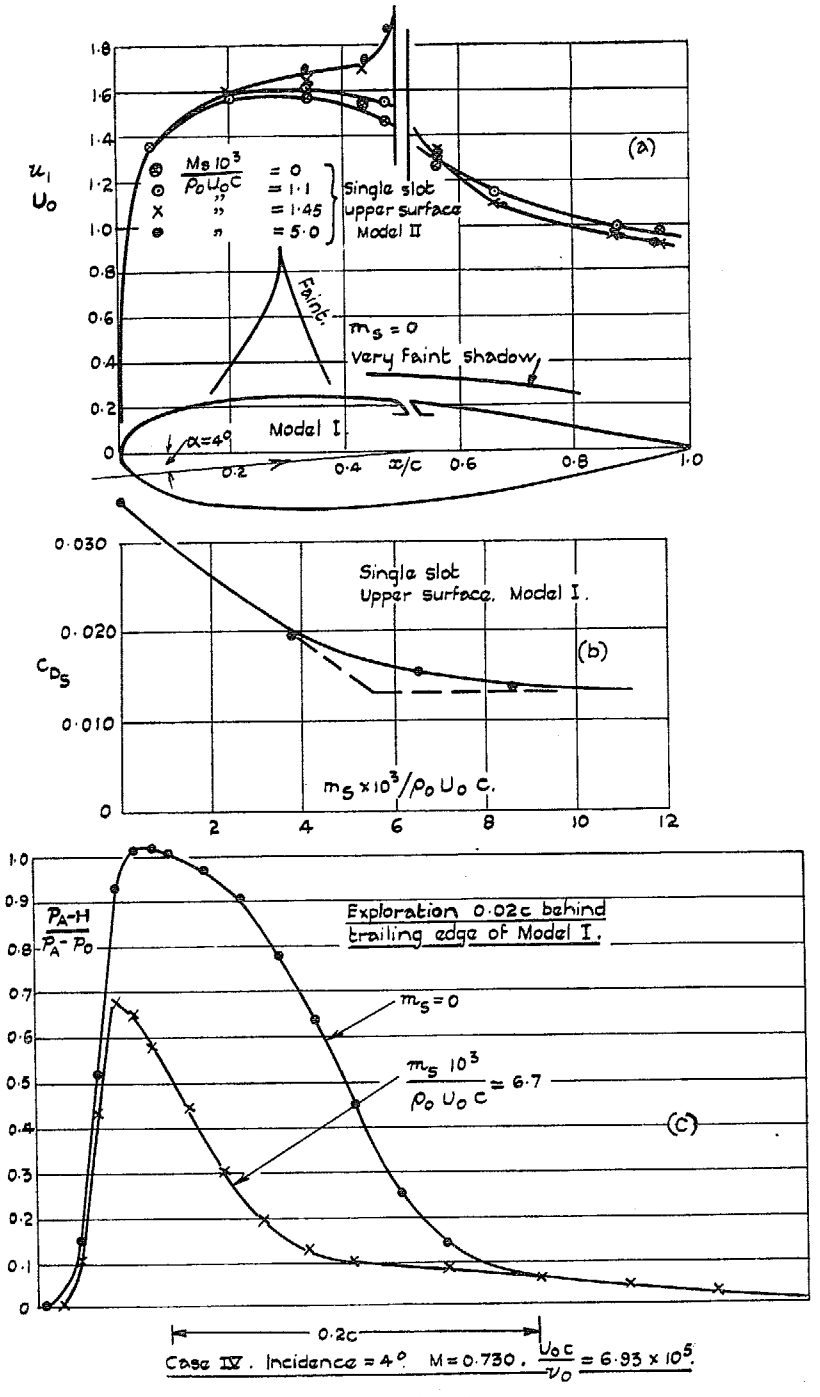

Case IV. Incidence = 4°. M = 0·730. $\frac{U_0 c}{\nu_0} = 6·93 \times 10^5$.

FIG. 6.

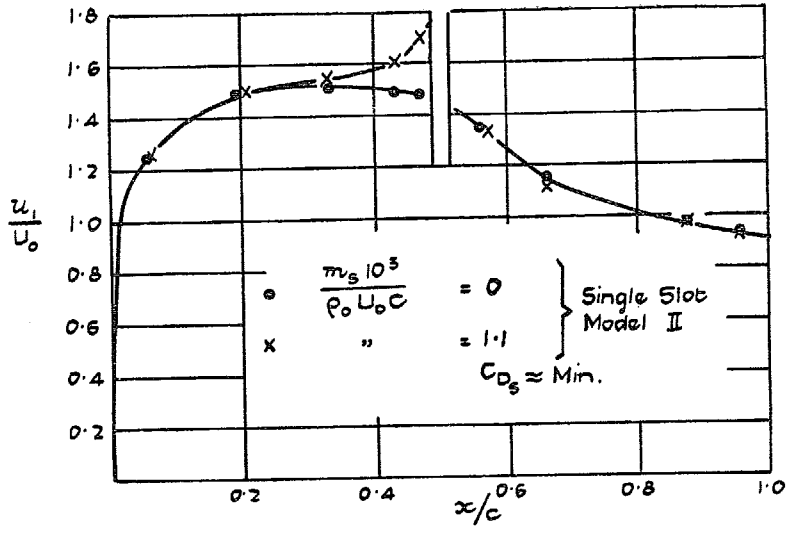

Incidence = 0° M = 0·745. $U_0 c/\nu_0 = 7·0 \times 10^5$.

FIG. 7.

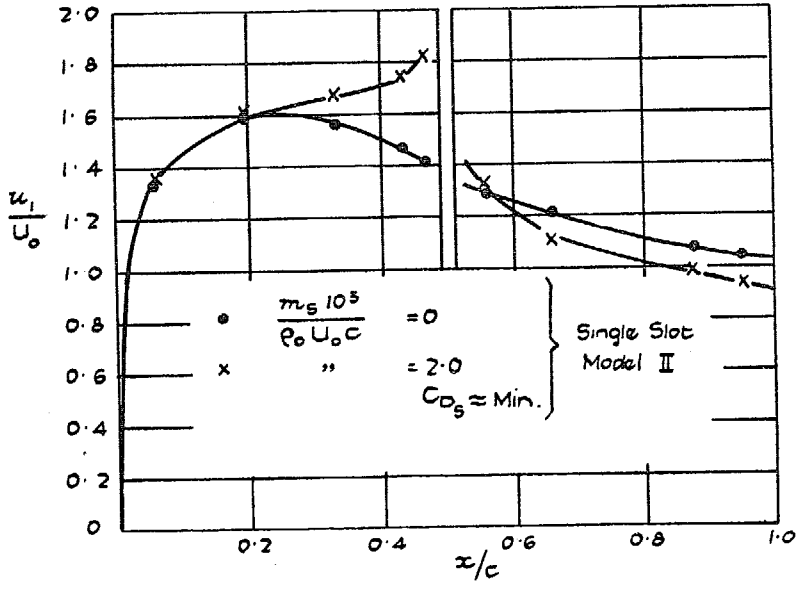

Incidence = 4°. M = 0·749. $U_0 c/\nu_0 = 7·0 \times 10^5$

FIG. 8.

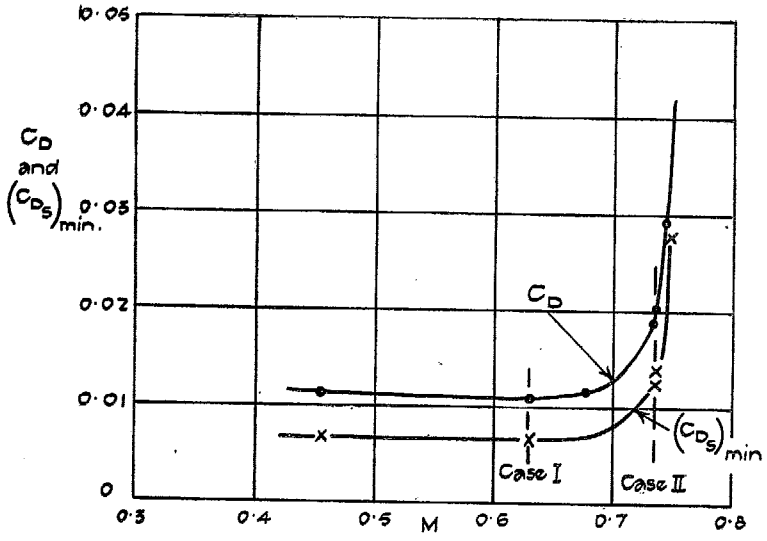

N A C A 0020. 0° Incidence. Model I. One Slot.

FIG. 9.

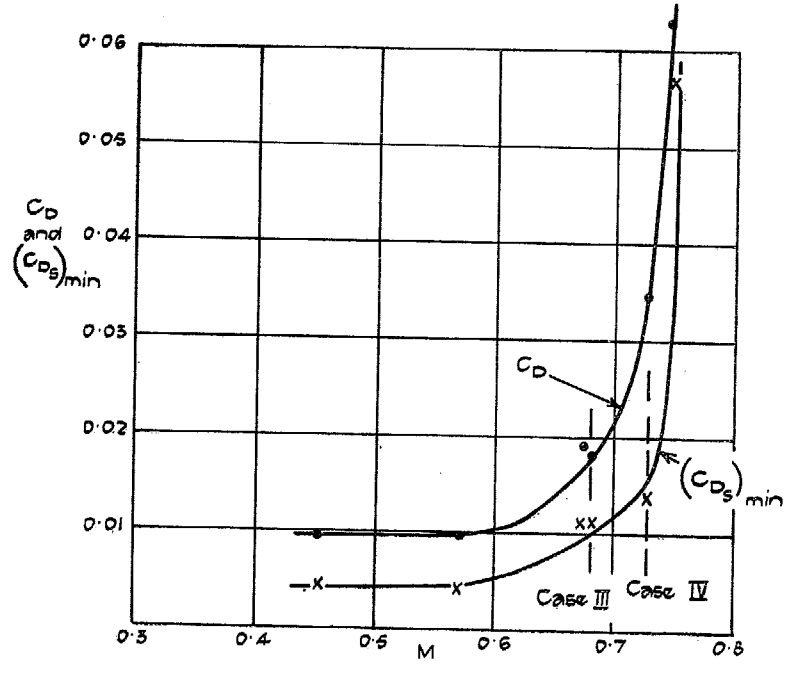

N A C A 0020. 4° Incidence Model I
Slot on Upper Surface.

FIG. 10.

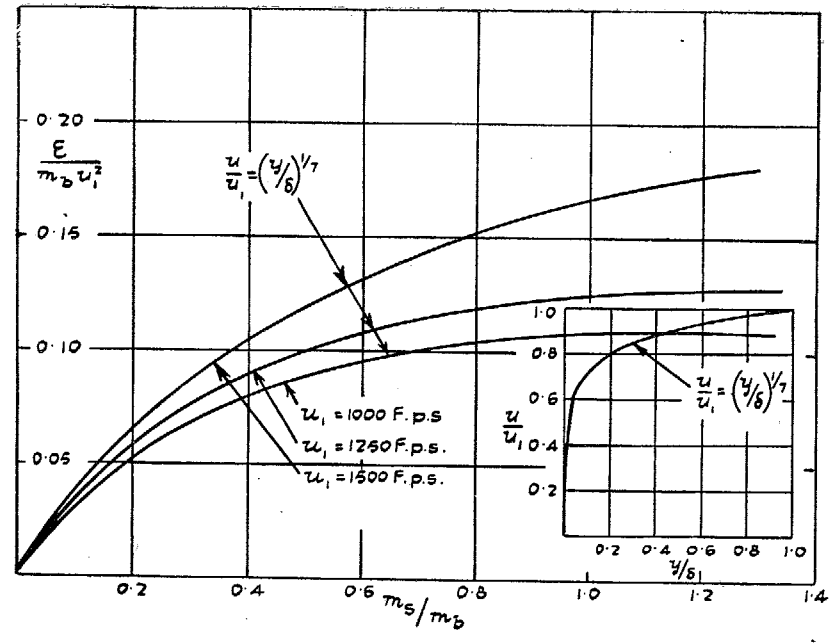

Turbulent Flow. a_0 = 1080 F.p.s. One Slot.

FIG. 11.

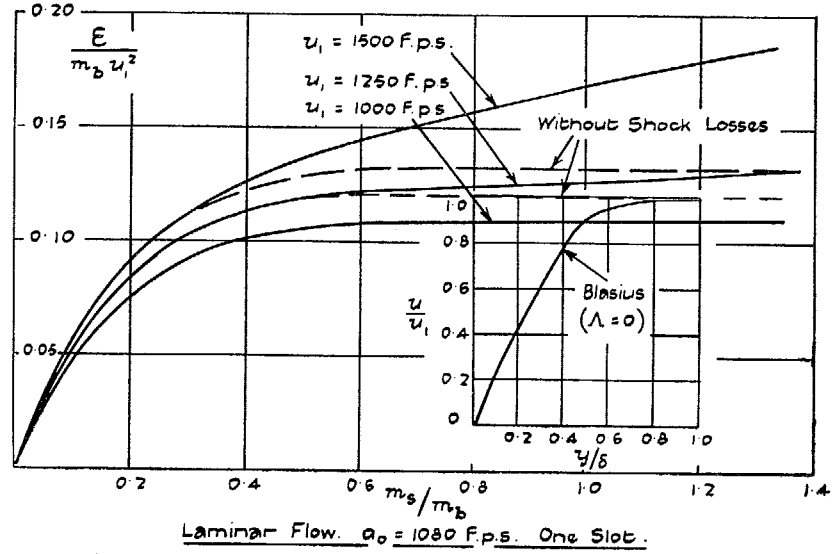

Laminar Flow. a_0 = 1080 F.p.s. One Slot.

FIG. 12.

(25528) Wt. 12/818 1/49 Hw.

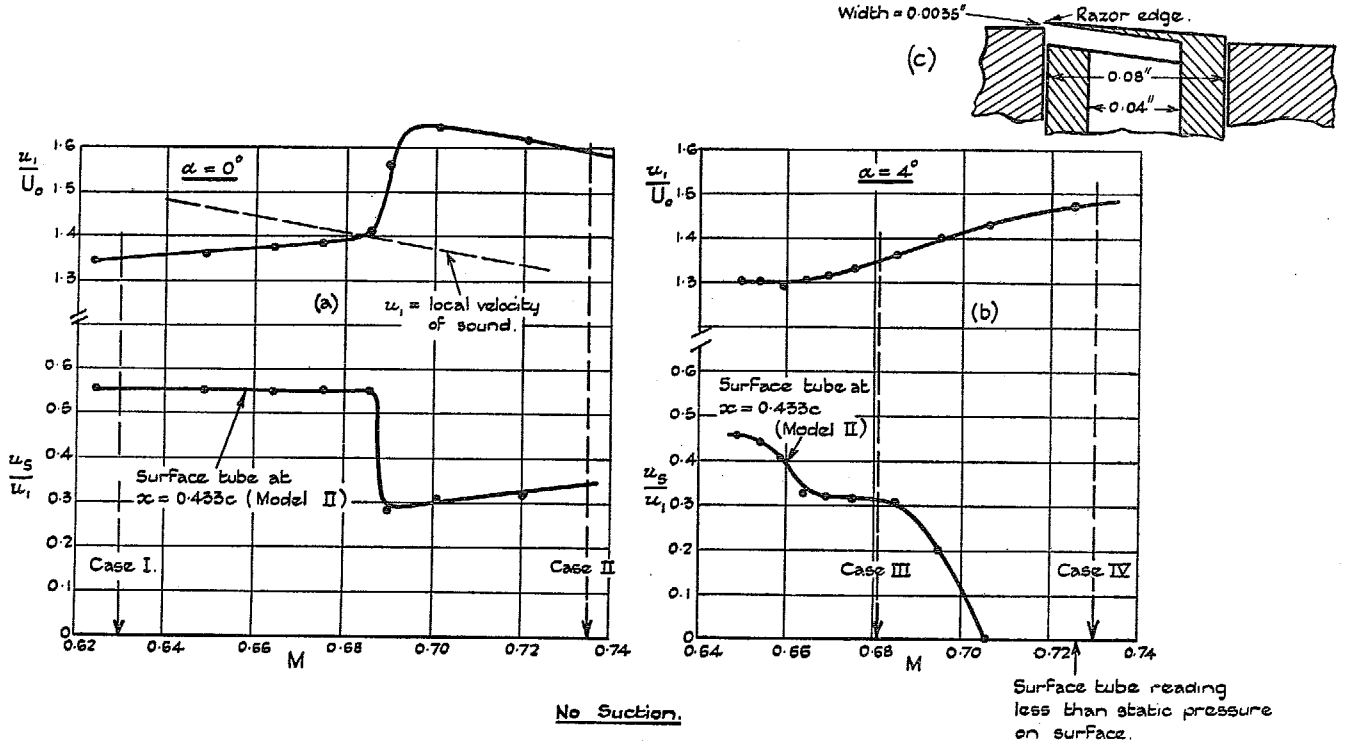

No Suction.

FIG. 13.

PRINTED IN GREAT BRITAIN

Publications of the Aeronautical Research Committee

TECHNICAL REPORTS OF THE AERONAUTICAL RESEARCH COMMITTEE—

1934-35 Vol. I. Aerodynamics. 40*s*. (40*s*. 8*d*.)
Vol. II. Seaplanes, Structures, Engines, Materials, etc. 40*s*. (40*s*. 8*d*.)

1935-36 Vol. I. Aerodynamics. 30*s*. (30*s*. 7*d*.)
Vol. II. Structures, Flutter, Engines, Seaplanes, etc. 30*s*. (30*s*. 7*d*.)

1936 Vol. I. Aerodynamics General, Performance, Airscrews, Flutter and Spinning. 40*s*. (40*s*. 9*d*.)
Vol. II. Stability and Control, Structures, Seaplanes, Engines, etc. 50*s*. (50*s*. 10*d*.)

1937 Vol. I. Aerodynamics General, Performance, Airscrews, Flutter and Spinning. 40*s*. (40*s*. 9*d*.)
Vol. II. Stability and Control, Structures, Seaplanes, Engines, etc. 60*s*. (61*s*.)

1938 Vol. I. Aerodynamics General, Performance, Airscrews, 50*s*. (51*s*.)
Vol. II. Stability and Control, Flutter, Structures, Seaplanes, Wind Tunnels, Materials. 30*s*. (30*s*. 9*d*.)

ANNUAL REPORTS OF THE AERONAUTICAL RESEARCH COMMITTEE—

1933-34 1*s*. 6*d*. (1*s*. 8*d*.)
1934-35 1*s*. 6*d*. (1*s*. 8*d*.)
April 1, 1935 to December 31, 1936. 4*s*. (4*s*. 4*d*.)
1937 2*s*. (2*s*. 2*d*.)
1938 1*s*. 6*d*. (1*s*. 8*d*.)

INDEXES TO THE TECHNICAL REPORTS OF THE ADVISORY COMMITTEE ON AERONAUTICS—

December 1, 1936 — June 30, 1939.	R. & M. No. 1850.	1*s*. 3*d*. (1*s*. 5*d*.)
July 1, 1939 — June 30, 1945.	R. & M. No. 1950.	1*s*. (1*s*. 2*d*.)
July 1, 1945 — June 30, 1946.	R. & M. No. 2050.	1*s*. (1*s*. 1*d*.)
July 1, 1946 — December 31, 1946.	R. & M. No. 2150.	1*s*. 3*d*. (1*s*. 4*d*.)
January 1, 1947 — June 30, 1947.	R. & M. No. 2250.	1*s*. 3*d*. (1*s*. 4*d*.)

Prices in brackets include postage.

Obtainable from

His Majesty's Stationery Office

London W.C.2 : York House, Kingsway
[Post Orders—P.O. Box No. 569, London, S.E.1.]
Edinburgh 2 : 13A Castle Street
Manchester 2 : 39 King Street
Birmingham 3 : 2 Edmund Street
Cardiff : 1 St. Andrew's Crescent
Bristol 1 : Tower Lane
Belfast : 80 Chichester Street
or through any bookseller.